

Decoherence dynamics of Majorana qubits under braiding operations

Hon-Lam Lai¹ and Wei-Min Zhang^{1,*}

¹*Department of Physics and Center for Quantum information Science,
National Cheng Kung University, Tainan 70101, Taiwan*

We study the decoherence dynamics of Majorana qubit braiding operations in a topological superconducting chain (TSC) system, in which the braiding is performed by controlling the electron-chemical potentials of the TSCs and the couplings between them. By solving rigorously the Majorana qubit dynamics, we show how the Majorana qubit coherence is generated through bogoliubon correlations formed by exchanging Majorana zero modes (MZMs) between two TSCs in braiding operations. Using the exact master equation, we demonstrate how MZMs and also the bogoliubon correlations dissipate due to charge fluctuations of the controlling gates at both the zero and finite temperatures. As a result, Majorana qubit coherence and the fermion parity conservation cannot be immune from local perturbations during braiding operations.

PACS numbers: 72.10.Bg, 73.63.-b, 85.30.Mn

Topological quantum computation (TQC) has recently attracted lots of attention as a promising candidate for the realization of quantum computation. Topological qubits consist of non-local degenerate ground states of Bogoliubov quasiparticles (bogoliubons) in topological superconductors, known as Majorana zero modes (MZMs) [1-3], and qubit operations are performed by braidings between MZMs [4-11]. It has been commonly believed that topological qubits have two main advantages [12]: (1) the qubit is protected by the fermion parity conservation in superconducting systems as long as perturbations are small compared to the energy gap between the MZMs and the non-zero energy bogoliubon states; (2) the two MZMs of each zero-energy bogoliubon are non-locally separated from each other so that topological qubits are considered to be immune to local perturbations during qubit manipulations.

However, the above picture of MZMs being robust against decoherence is only an ideal thought. In reality, performing braidings of MZMs inevitably leads to couplings between the MZMs and the controlling gates. In other words, topological qubits must be influenced from various environment noises, and the above two advantages of topological qubits should be reexamined in the open quantum system perspective. It is easy to understand that coupling MZMs to an ungapped fermionic bath could break the fermion parity conservation because electrons can tunnel into the bath without energy cost [13]. Even when the MZMs is coupled to a gapped fermionic bath through a bosonic field, electrons can still overcome the energy gap and tunnel to the bath due to the bosonic field fluctuation [14, 15]. In our recent work, we applied our exact master equation to a TSC system subjected to charge fluctuations of a controlling gate and studied the exact non-Markovian decoherence dynamics of MZMs [16]. We found that at zero temperature, there is a localized bound state located at zero energy due to the particle-hole symmetry that can partially protect the MZM from decoherence. At any low but finite

temperature, MZMs can be locally destroyed completely.

We shall study in this Letter the non-local feature of the MZMs through the braiding operations, which is crucial for the realization of topological quantum computers. Qubit information cannot be encoded in the two degenerate states of one single zero-energy bogoliubon due to the parity conservation. Therefore, at least four MZMs (two bogoliubons) must be involved in encoding quantum information. More specifically, two bogoliubons correlate to each other to encode non-locally qubit information in the same parity sector through the braiding operation of MZMs. We find that local perturbations to a single MZM can destroy the correlation between different bogoliubons and thus destroy the quantum information encoded in the topological qubit. Therefore, even though local perturbations to a single MZM cannot affect the wavefunction of another spatially separated MZM of the same bogoliubon, this does not imply the protection of topological qubit information from local perturbations. In fact, as we shall show in this Letter, Majorana qubit coherence is generated through the formation of bogoliubon correlation between different TSCs, and local perturbations that destroy bogoliubon correlations will naturally destroy the Majorana qubit coherence in topological quantum computations.

Because of the close relation between bogoliubon correlations and qubit coherence, we study explicitly Majorana qubit decoherence through the exploration of the decoherence dynamics of bogoliubon correlations in braiding operations. More specifically, we study the Majorana qubit decoherence dynamics under direct braiding of MZMs in a quasi-1D network with the exact master equation in this Letter. Braidings of MZMs in quasi-1D networks can be realized by tuning the chemical potentials of TSCs and the coupling potentials between them. The chemical potentials of TSCs can be tuned by “keyboard” gates that individually control the electron-chemical potentials at different parts of the network [4]. The coupling potentials between different TSCs can be tuned by gates

that control the tunneling barriers between MZMs [6-8]. We treat the T-junction-TSC system as an open quantum system, in which the MZMs can be moved by braiding through controlling gates. We then solve the Majorana correlation functions and the reduced density matrix of the Majorana qubit in the real-time domain in which all the non-Markovian effects are fully taken into account, and from which we explore explicitly how braiding operations of MZMs generates Majorana qubit coherence and how non-adiabatic braiding operation and the associated charge-fluctuation induced decoherence take place.

Majorana braiding and non-adiabatic decoherence dynamics. We begin with a T-junction consisting of three TSCs (see Fig. 1), each TSC is modeled by effective p -wave spinless superconductor Hamiltonians [12-22]

$$\begin{aligned}
 H_{\text{TSC}}^{\alpha} &= \sum_i \left[-\frac{\Delta_{\alpha,i}}{2} c_{\alpha,i+1} c_{\alpha,i} - \frac{w_{\alpha,i}}{2} c_{\alpha,i+1}^{\dagger} c_{\alpha,i} + \text{H.c.} \right. \\
 &\quad \left. + \mu_{\alpha,i} c_{\alpha,i}^{\dagger} c_{\alpha,i} \right] \\
 &= -i \sum_{i=1}^{N/2-1} \frac{w}{2} \gamma_{\alpha,2i} \gamma_{\alpha,2i+1} + i \sum_{i=1}^{N/2} \frac{\mu_{\alpha,i}}{2} \gamma_{\alpha,2i-1} \gamma_{\alpha,2i},
 \end{aligned} \quad (1)$$

where $c_{\alpha,i}^{\dagger}$ ($c_{\alpha,i}$) is the creation (annihilation) operator of electrons at site i of TSC α ($\alpha = L, R, M$), $\Delta_{\alpha,i}$ and $w_{\alpha,i}$ are the pairing and hopping amplitudes respectively, and $\mu_{\alpha,i}$ is the electron-chemical potential. The Majorana operators $\gamma_{\alpha,2i-1} = c_{\alpha,i} + c_{\alpha,i}^{\dagger}$ and $\gamma_{\alpha,2i} = -i(c_{\alpha,i} - c_{\alpha,i}^{\dagger})$. For simplicity, we set $\Delta_{\alpha,i} = w_{\alpha,i} = w$ hereafter. The coupling Hamiltonian between the left and middle TSCs and between the middle and right TSCs is given by

$$H_{\text{T}}(t) = i \frac{w_{LM}(t)}{2} \gamma_{L,2N} \gamma_{M,1} + i \frac{w_{RM}(t)}{2} \gamma_{R,2N} \gamma_{M,1}, \quad (2)$$

where $w_{L(R)M}$ is the coupling amplitude between two Majorana sites located at the left (right) and the middle TSCs. The electron-chemical potentials of the left and right TSCs are set to be zero ($\mu_{L,i} = \mu_{R,i} = 0$) so that both TSCs are kept in topological phase. The electron-chemical potentials of the middle TSC are prepared so that $\mu_{M,1} = \mu(t)$ and $\mu_{M,i>1} \gg \Delta_{M,i}$, namely, the electron-chemical potential at site 1 can be individually tuned freely by a controlling gate [4], while all other sites are kept in non-topological phase. As a result, initially four MZMs in the left and right TSCs at sites $\gamma_{L,1}$, $\gamma_{L,2N}$, $\gamma_{R,1}$ and $\gamma_{R,2N}$, see Fig. 1(a), are formed the topological qubit space under consideration.

Consider the even-parity state space of the four MZMs as the topological qubit with the basis $|00\rangle$ and $|11\rangle = b_L^{\dagger} b_R^{\dagger} |00\rangle$. The system is prepared initially in one of the degenerate ground states $|11\rangle$. The empty state $|00\rangle$ is annihilated by the left and right TSCs zero-energy bogoliubon operators b_L and b_R , which are defined as $b_L = \gamma_{L,1} + i\gamma_{L,2N}$ and $b_R = \gamma_{R,1} + i\gamma_{R,2N}$. In

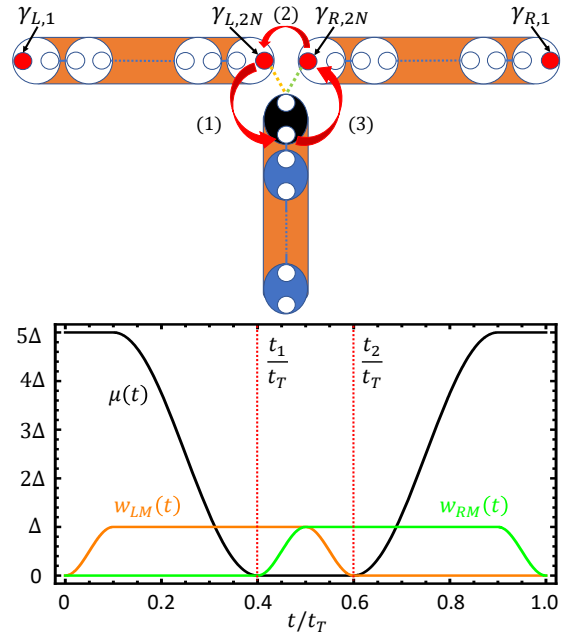


FIG. 1: (Colour online) (a) (Top) Three TSCs form a T-junction with four MZMs at sites $\gamma_{L,1}$, $\gamma_{L,2N}$, $\gamma_{R,1}$ and $\gamma_{R,2N}$ respectively. Braiding operation is performed in three steps (1), (2) and (3) by tuning the chemical potential $\mu(t)$ of the middle TSC and the couplings $w_{LM}(t)$ and $w_{RM}(t)$ of the left TSC and the right TSC with the middle TSC, respectively. (b) (Bottom) Changes of parameters in a braiding process: $\mu_{M,1}(t)$ (black), $w_{LM}(t)$ (orange) and $w_{RM}(t)$ (green).

other words, initially the MZMs at sites $\gamma_{L,1}$ ($\gamma_{R,1}$) and $\gamma_{L,2N}$ ($\gamma_{R,2N}$) are paired to form a zero-energy bogoliubon. The braiding is performed between the MZMs at sites $\gamma_{L,2N}$ and $\gamma_{R,2N}$, by tuning the chemical potential $\mu_{M,1}(t)$ of the middle TSC and the couplings $w_{LM}(t)$ and $w_{RM}(t)$ between the left TSC with the middle TSC, respectively, see Fig. 1b. The detailed dynamics of this braiding operation is manifested in the correlation functions of different Majorana sites, as shown in Fig. 2. As one can see in Fig. 2a, the correlation functions $i\langle\gamma_{L,1}(t)\gamma_{L,2N}(t)\rangle$ and $i\langle\gamma_{R,1}(t)\gamma_{R,2N}(t)\rangle$ gradually decrease to zero while $i\langle\gamma_{L,1}(t)\gamma_{R,2N}(t)\rangle$ and $i\langle\gamma_{L,2N}(t)\gamma_{R,1}(t)\rangle$ increase to unity. In the end of braiding operation, it realizes the exchange of $\gamma_{L,2N} \leftrightarrow \gamma_{R,2N}$, see an intuitive derivation in the Supplemental Materials [23]. This exchange of correlations between the Majorana sites at the left and right TSCs shows that the two zero-energy bogoliubons b_L and b_R become correlated to each other due to the braiding operation.

The correlation between two zero-energy bogoliubons directly generates the Majorana qubit coherence, as can be observed from the qubit density matrix element $\rho_{11,00} = \langle b_L(t)b_R(t) \rangle$, where the qubit is initially in the state $|11\rangle$, and after the braiding operation, it becomes $(|00\rangle + |11\rangle)/\sqrt{2}$, a qubit superposition state, as shown in Fig. 2b. On the other hand, during the braiding

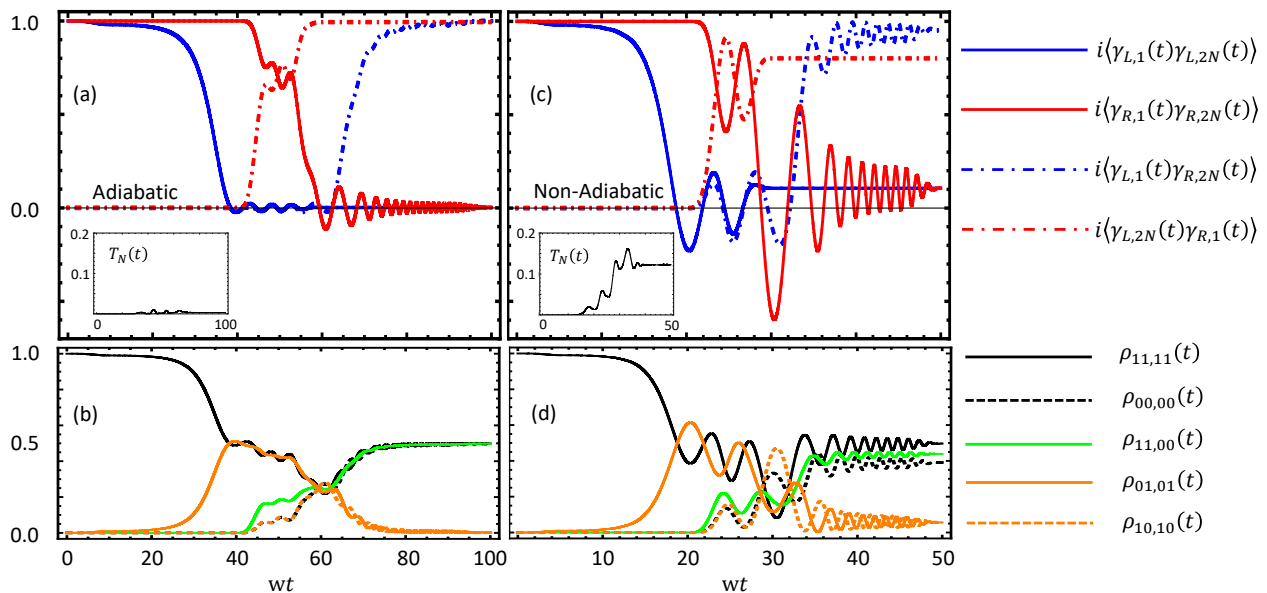


FIG. 2: (Colour online) (a) (Top left) Time evolution of correlation functions with total operation time $wt_T = 100$. (b) (Bottom left) Time evolution of density matrix elements with total operation time $wt_T = 100$. (Inserted) Excitation number of zero-energy bogoliubons $T_N(t)$. (c) (Top right) Time evolution of correlation functions with total operation time $wt_T = 50$. (d) (Bottom right) Time evolution of density matrix elements with total operation time $wt_T = 50$. (Inserted) Excitation number of zero-energy bogoliubons $T_N(t)$.

operation, the closure of the even-parity qubit space is temporarily broken, as indicated by the non-vanishing values of density matrix elements $\rho_{01,01}(t)$ and $\rho_{10,10}(t)$. This is because one of the MZMs must be moved to the middle TSC in order to complete the braiding operation. At the end both $\rho_{01,01}$ and $\rho_{10,10}$ vanish, indicating that the left and right TSCs system are maintained in the even-parity state space. Also $\rho_{00,00} = \rho_{11,11} = \rho_{11,00}$ indicating a perfect realization of Majorana qubit coherence.

The results of Fig. 2a, b are obtained by slowly tuning the parameter $\mu(t)$, $w_{LM}(t)$ and $w_{RM}(t)$, as shown in Fig. 1b with $t_T = 100/w$. To examine the non-adiabatic effects of the braiding operation, the same braiding procedure is repeated with a shorter operation time (take here, for example, $t_T = 50/w$ in Fig. 1b). Firstly, notice

the non-adiabatic charactering function $T_N(t)$ (defined in the Supplementary materials [23]) which describes the number of zero-energy bogoliubon being excited to the non-zero energy bogoliubon state due to non-adiabatic effect (see the inserted panel in Fig. 2c). Secondly, one can see from Fig. 2c that the exchange of MZMs between Majorana sites $\gamma_{L,2N}$ and $\gamma_{R,2N}$ cannot be completed because the controlling parameters are changed too fast (see Fig. 2c). As a result, the left and right bogoliubons are only partially correlated and the qubit coherence is not fully generated (see Fig. 2d). The fermion parity conservation is also broken, as shown by the non-vanished values of the old-parity matrix elements $\rho_{10,10}$ and $\rho_{01,01}$ in the steady-state limit shown in Fig. 2d, due to the non-adiabatic excitations.

Decoherence Dynamics Due to Charge Fluctuations. In order to control the electron-chemical potential, a controlling gate is applied and we shall consider how charge fluctuations of the controlling gate affect the braiding operation. The total Hamiltonian incorporating charge fluctuations is given by [15]

$$H = \sum_{\alpha=L,M,R} H_{\text{TSC}}^{\alpha}(t) + H_{\text{T}}(t) + H_G + H_C, \quad (3)$$

where H_G is the Hamiltonian of the controlling gate,

which is modeled by a non-interacting electron gas, $H_G = \sum_p \epsilon_p c_p^{\dagger} c_p$, where c_p^{\dagger} (c_p) is the creation (annihilation) operator of an electron in the gate with energy ϵ_p , and H_C is the coupling Hamiltonian between the TSC and the gate,

$$H_C = \sum_{\alpha=L,M,R} \eta_{\alpha} \delta Q_{\alpha} \sum_i F_{\alpha,i} c_{\alpha,i}^{\dagger} c_{\alpha,i}, \quad (4)$$

in which $c_{\alpha,i}^{\dagger}$ ($c_{\alpha,i}$) is the creation (annihilation) operator of an electron at site i of the TSC α [see Eq. (1)], η_{α} is

the coupling parameter, δQ_α is the charge fluctuation of the gate and $F_{\alpha,n}$ is a profile function which limits the range of the chain α affected by the gate, and one can set $F_{\alpha,n}$ equals to unity if site n is near the TSC junction and zero otherwise. For simplicity, we assume that all the controlling gates are identical so that we can omit the subscript α hereafter. The spectral density function of the charge fluctuation of the gate is given by

$$J_C(\omega) = B_C \exp\left(-\frac{\omega^2}{8E_F\omega_c}\right) \frac{\omega}{1 - e^{-\omega/kT}}, \quad (5)$$

where E_F is the fermi energy of the controlling gate, kT is the temperature of the gate, ω_c is a cut-off frequency of charge fluctuations, and B_C is a factor determined by the structure of the gate [15].

We extend our previous work of the exact master equation for Majorana zero modes [16] to the topological qubit density matrix $\rho(t)$, which is given by

$$\begin{aligned} \frac{d}{dt}\rho(t) = & \Gamma_L(t, t_0)[\gamma_{L,2N}\rho(t)\gamma_{L,2N} - \rho(t)] \\ & + \Gamma_R(t, t_0)[\gamma_{R,2N}\rho(t)\gamma_{R,2N} - \rho(t)] \\ & + \Theta(t, t_0)[\gamma_{L,2N}\rho(t)\gamma_{R,2N} + \gamma_{R,2N}\rho(t)\gamma_{L,2N}] \\ & + \Lambda(t, t_0)[\gamma_{L,2N}\gamma_{R,2N}\rho(t) + \rho(t)\gamma_{R,2N}\gamma_{L,2N}] \\ & + \tilde{\Lambda}(t, t_0)[\gamma_{L,2N}\gamma_{R,2N}\rho(t) - \rho(t)\gamma_{R,2N}\gamma_{L,2N}]. \end{aligned} \quad (6)$$

The time-dependent coefficients $\Gamma_{L(R)}(t, t_0)$, $\Theta(t, t_0)$, $\Lambda(t, t_0)$ and $\tilde{\Lambda}(t, t_0)$ are given in the Supplementary materials.

We perform the same braiding procedure as in the previous section under the charge fluctuations of the gates. Fig. 3 shows the decoherence dynamics of the TSC-system density matrix elements at various coupling regimes for both the zero temperature and finite temperature ($kT = 0.5w$). First of all, MZMs at sites $\gamma_{L,2N}$ and

$\gamma_{R,2N}$ are subjected to the charge fluctuation, leading to the dissipation of the corresponding bogoliubon correlations. As we have mentioned above, the qubit coherence is generated through the formation of bogoliubon correlations between the two TSCs so that the dissipation of MZMs will lead to the destruction of qubit coherence, as illustrated by $\rho_{11,00}(t)$ in Fig. 3. At zero temperature, the MZMs are partially protected by the localized bound states due to the particle-hole symmetry [16], part of the bogoliubon correlations can still be formed in the braiding operation so that the qubit coherence is partially generated and preserved (see Fig. 3a, c, e). In contrast, at finite temperature, the localized bound states do not exist and the fluctuation-affected MZMs eventually decay to zero [16]. In particular, in the weak coupling regime ($\frac{\pi}{2}B_C\eta^2 < 0.5$), the MZMs decay comparatively slower so that the bogoliubon correlations can still be formed in the braiding process, thus the qubit coherence can be partially generated before it decays to zero (see Fig. 3b, d). However, in the strong coupling regime ($\frac{\pi}{2}B_C\eta^2 = 1$), the MZMs decay so quickly that the bogoliubon correlations cannot be formed during the braiding process. Therefore, qubit coherence cannot be generated at all in the strong coupling regime (see Fig. 3f).

Secondly, the fermion parity conservation and thus the closure of the qubit state space are also broken by charge fluctuations. The qubit density matrix elements $\rho_{01,01}(t)$ and $\rho_{10,10}(t)$ describe the bogoliubon occupation number in the odd-parity state space, their non-vanishing values indicate the breakdown of the parity-conserved qubit space. At zero temperature, the localized bound states suppress the breakdown of the fermion parity conservation (see Fig. 3a, c, e). While at finite temperature, two bogoliubons (four MZMs) eventually evolve into a totally mixed state (see Fig. 3b, d, f).

In conclusion, we have studied the decoherence dynamics of a Majorana qubit under braiding operation in a T-junction-TSC system with the exact master equation. During the braiding process, two MZMs in the right and left sides of two TSCs exchange so that two zero-energy bogoliubons become correlated to each other. The Majorana qubit coherence is generated through this correlation formation between two bogoliubons in different TSCs. We show that non-adiabatic decoherence will damage the qubit coherence because of the incomplete formation of bogoliubon correlation. It also breaks the fermion parity conservation because of the non-adiabatic excitations. When charge fluctuations induced from the controlling gate are taken into account, the fluctuation-affected MZMs in both TSCs will dissipate. As a result,

in the weak coupling regime, the qubit coherence is only partially generated in the beginning of the braiding operation, and then the coherence decays away eventually. While in the strong coupling regime, the qubit coherence cannot be generated at all. Also we show that at finite temperature, the four MZMs eventually become a totally mixed state so that the information encoded in the Majorana qubit is completely lost in topological quantum computations. These results show that the advantages of Majorana qubits from the non-locality and the fermion parity conservation are destroyed by local perturbations.

We acknowledge the support from the Ministry of Science and Technology of Taiwan under Contract Nos. NSC-105-2112-M-006-008-MY3 and NSC-108-2112-M-006-009-MY3.

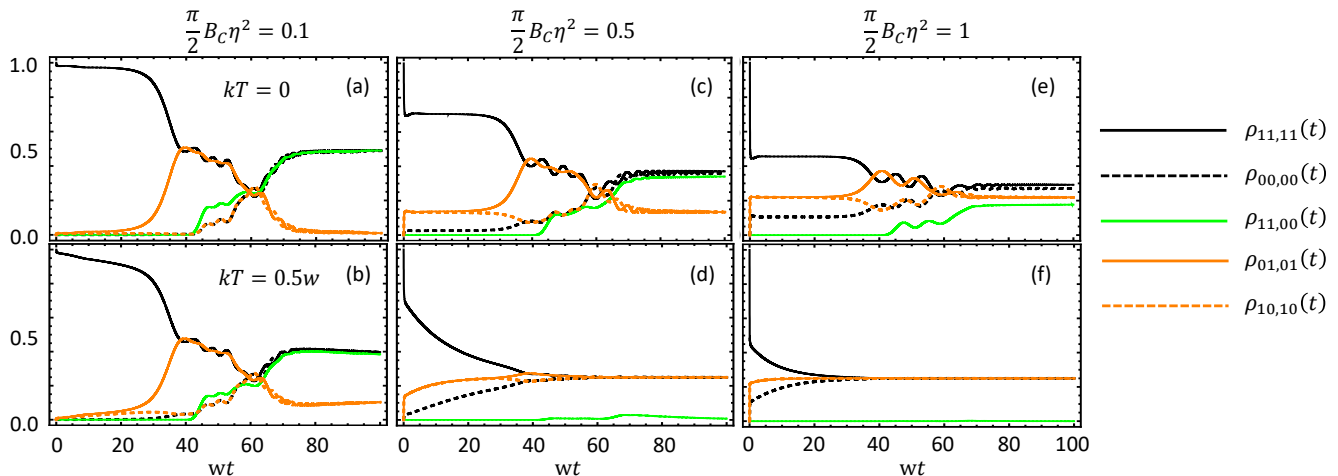


FIG. 3: (Colour online) Time evolution of density matrix elements with (a) (top left) $\frac{\pi}{2} B_C \eta^2 = 0.1$, $kT = 0$, (b) (bottom left) $\frac{\pi}{2} B_C \eta^2 = 0.1$, $kT = 0.5w$, (c) (top middle) $\frac{\pi}{2} B_C \eta^2 = 0.5$, $kT = 0$, (d) (bottom middle) $\frac{\pi}{2} B_C \eta^2 = 0.5$, $kT = 0.5w$, (e) (top right) $\frac{\pi}{2} B_C \eta^2 = 1$, $kT = 0$, (f) (bottom right) $\frac{\pi}{2} B_C \eta^2 = 1$, $kT = 0.5w$, with initial qubit state $|11\rangle$.

* Electronic address: wzhang@mail.ncku.edu.tw

- [1] A. Kitaev, *Fault-tolerant quantum computation by anyons*, Ann. Phys. **303**, 2 (2003).
- [2] M. Freedman, A. Kitaev, M. J. Larsen, and Z. Wang, *Topological quantum computation*, Bull. Am. Math. Soc. **40**, 31-38 (2003).
- [3] C. Nayak, S. H. Simon, A. Stern, M. Freedman, and S. Das Sarma, *Non-Abelian anyons and topological quantum computation*, Rev. Mod. Phys. **80**, 1083 (2008).
- [4] J. Alicea, Y. Oreg, G. Refael, F. von Oppen and M. P. A. Fisher, *Non-Abelian statistics and topological quantum information processing in 1D wire networks*, Nature Physics **7**, 412-417 (2011).
- [5] D. Aasen, M. Hell, R. V. Mishmash, A. Higginbotham, J. Danon, M. Leijnse, T. S. Jespersen, J. A. Folk, C. M. Marcus, K. Flensberg, and J. Alicea, *Milestones toward Majorana-based quantum computing*, Phys. Rev. X **6**, 031016 (2016).
- [6] J. D. Sau, S. Tewari, and S. D. Sarma, *Universal quantum computation in a semiconductor quantum wire network*, Phys. Rev. A **82**, 052322 (2010).
- [7] J. D. Sau, D. J. Clarke, and S. Tewari, *Controlling non-Abelian statistics of Majorana fermions in semiconductor nanowires*, Phys. Rev. B, **84**, 094505 (2011).
- [8] B. van Heck, A. R. Akhmerov, F. Hassler, M. Burrello, and C. W. J. Beenakker, *Coulomb-assisted braiding of Majorana fermions in a Josephson junction array*, New Journal of Phys. **14**, (2012).
- [9] P. Bonderson, M. Freedman, and C. Nayak, *Measurement-Only Topological Quantum Computation*, Phys. Rev. Lett. **101**, 010501 (2008).
- [10] T. Hyart, B. van Heck, I. C. Fulga, M. Burrello, A. R. Akhmerov, and C. W. J. Beenakker, *Flux-controlled quantum computation with Majorana fermions*, Phys. Rev. B **88**, 035121 (2013).
- [11] T. Karzig, C. Knapp, R. M. Lutchyn, P. Bonderson, M. B. Hastings, C. Nayak, J. Alicea, K. Flensberg, S. Plugge, Y. Oreg, C. M. Marcus, and M. H. Freedman, *Scalable designs for quasiparticle-poisoning-protected topological quantum computation with Majorana zero modes*, Phys. Rev. B **95**, 235305 (2017).
- [12] A. Kitaev, *Unpaired Majorana Fermions in Quantum wires*, Phys. Usp. **44**, 131 (2001).
- [13] J. C. Budich, S. Walter, and B. Trauzettel, *Failure of protection of Majorana based qubits against decoherence*, Phys. Rev. B **85**, 121405 (2012).
- [14] G. Goldstein and C. Chamon, *Decay rates for topological memories encoded with Majorana fermions*, Phys. Rev. B **84**, 205109 (2011).
- [15] M. J. Schmidt, D. Rainis, and D. Loss, *Decoherence of Majorana qubits by noisy gates*, Phys. Rev. B **86**, 085414 (2012).
- [16] H. L. Lai, P. Y. Yang, Y. W. Huang, and W. M. Zhang, *Exact master equation and non-Markovian decoherence dynamics of Majorana zero modes under gate-induced charge fluctuations*, Phys. Rev. B **97**, 054508 (2018).
- [17] L. Fu, and C. L. Kane, *Superconducting proximity effect and Majorana fermions at the surface of a topological insulator*, Phys. Rev. Lett. **100**, 096407 (2008).
- [18] J. Linder, Y. Tanaka, T. Yokoyama, A. Sudbø, and N. Nagaosa, *Unconventional superconductivity on a topological insulator*, Phys. Rev. Lett. **104**, 040502 (2010).
- [19] J. D. Sau, R. M. Lutchyn, S. Tewari, and S. Das Sarma, *Generic new platform for topological quantum computation using semiconductor heterostructures*, Phys. Rev. Lett. **104**, 067001 (2010).
- [20] R. M. Lutchyn, J. D. Sau, and S. Das Sarma, *Majorana fermions and a topological phase transition in semiconductor-superconductor heterostructures*, Phys. Rev. Lett. **105**, 077001 (2010).
- [21] Y. Oreg, G. Refael, and F. von Oppen, *Helical liquids and Majorana bound states in quantum wires*, Phys. Rev. Lett. **105**, 177002 (2010).
- [22] S. M. Albrecht, A. P. Higginbotham, M. Madsen, F. Kuemmeth, T. S. Jespersen, J. Nygard, P. Krogstrup, and C. M. Marcus, *Exponential protection of zero modes in Majorana islands*, Nature **531**, 206 (2016).

[23] see Supplemental Materials,